where the partition coefficient becomes comparable to 1 and is less and less sensitive to concentration. For a more definite confirmation of this point, it should be necessary to perform experiments at higher R_H/R_p value.

The presence of the diffusional boundary layer limits the accuracy of the determination of the true diffusion coefficient through the membrane. Its influence is minimized at low porosity at the cost of longer duration of the diffusion experiments.

Registry No. Polystyrene, 9003-53-6; bisphenol A polycarbonate (copolymer), 25037-45-0; bisphenol A polycarbonate (SRU), 24936-68-3.

References and Notes

(1) Satterfield, C. N.; Colton, C. K.; Pitcher, W. H. *AIChE J.* **1975**, *21*, 289.
(2) Haller, W. *Macromolecules* **1977**, *10*, 83.
(3) Beck, R. E.; Schulz, S. J. *Biochim. Biophys. Acta* **1972**, *255*, 273.
(4) (a) Long, T. D.; Jacobs, D. L.; Anderson, J. L. *J. Membr. Sci.* **1981**, *9*, 13. (b) Baltus, R. E.; Anderson, J. L. *Chem. Eng. Sci.* **1983**, *38*, 1959.
(5) Bohrer, M. P.; Patterson, G. D.; Carroll, P. J. *Macromolecules* **1984**, *17*, 1170.
(6) Renkin, E. M. *J. Gen. Physiol.* **1954**, *38*, 225.
(7) Bean, C. P. In *Membranes, A Series of Advances*; Eisenman, G., Ed.; Wiley: New York, 1972, Vol. 1.
(8) Giddings, J. C.; Kucera, E.; Russell, C. P.; Myers, M. N. *J. Phys. Chem.* **1968**, *72*, 4397.
(9) Anderson, J. L.; Quinn, J. A. *Biophys. J.* **1974**, *14*, 130.
(10) (a) Casassa, E. F. *J. Polym. Sci., Part B* **1967**, *5*, 773. (b) Casassa, E. F.; Tagami, Y. *Macromolecules* **1969**, *2*, 14. (c) Casassa, E. F. *Macromolecules* **1976**, *9*, 182.
(11) Satterfield, C. N.; Colton, C. K.; de Turckeim, B.; Copeland, T. M. *AIChE J.* **1978**, *24*, 937.
(12) Schulz, J. S.; Valentine, R.; Choi, C. Y. *J. Gen. Physiol.* **1979**, *73*, 49.
(13) Long, T. D.; Anderson, J. L. *J. Polym. Sci., Polym. Phys. Ed.* **1984**, *22*, 1261.
(14) (a) Chauveteau, G.; Tirrell, M.; Omari, A. *J. Colloid Interface Sci.* **1984**, *100*, 41. (b) Nguyen, Q., T.; Néel, J. *J. Membr. Sci.* **1983**, *14*, 97, 111.
(15) Cannell, D.; Rondelez, F. *Macromolecules* **1980**, *13*, 1599.
(16) Guillot, G.; Léger, L.; Rondelez, F. *Macromolecules* **1985**, *18*, 2531.
(17) Daoudi, S.; Brochard, F. *Macromolecules* **1978**, *11*, 751.
(18) De Gennes, P.-G. In *Scaling Concepts in Polymer Physics*; Cornell University: Ithaca, NY, 1979.
(19) Munch, J. P.; Candau, S.; Herz, J.; Hild, G. *J. Phys. (Les Ulis, Fr.)* **1977**, *38*, 971.
(20) (a) Schick, M. J.; Doty, P.; Zimm, B. H. *J. Am. Chem. Soc.* **1950**, *72*, 530. (b) Jacobsson, G. *Acta Chem. Scand.* **1954**, *8*, 1843. (c) Vink, H. *Eur. Polym. J.* **1974**, *10*, 149.
(21) Guillot, G. *Macromolecules*, following paper in this issue.
(22) Guillot, G.; Rondelez, F. *J. Appl. Phys.* **1981**, *52*, 7155.
(23) Léger, L.; Hervet, H.; Rondelez, F. *Macromolecules* **1981**, *14*, 1732.
(24) Lesec, J. Ecole Supérieure de Physique et Chimie, Paris, private communication.
(25) (a) Malone, D. M.; Anderson, J. L. *AIChE J.* **1977**, *23*, 177. (b) Keller, K. H.; Stein, T. T. *Math. Biosci.* **1967**, *1*, 421.
(26) (a) Odell, J. A.; Keller, A.; Miles, M. J. *Polym. Commun.* **1983**, *24*, 7. (b) Munch, W. D.; Zestar, L. P.; Anderson, J. L. *J. Membr. Sci.* **1979**, *77*, 102.
(27) Bohrer, M. P. *Ind. Eng. Chem. Fundam.* **1983**, *22*, 72.
(28) Guillot, G. Thèse Université Paris-Sud, Orsay, 1986.
(29) Zemans, L.; Wales, M. *Sep. Sci. Technol.* **1981**, *16*, 275.
(30) Daoud, M.; de Gennes, P. G. *J. Phys. (Les Ulis, Fr.)* **1977**, *38*, 85.
(31) Brochard, F.; de Gennes, P.-G. *J. Chem. Phys.* **1977**, *67*, 52.
(32) (a) Flory, P. J. *Principles of Polymer Chemistry*; Cornell University Press: Ithaca, NY, 1978. (b) Tanford, C. *Physical Chemistry of Macromolecules*; Wiley: New York, 1968.
(33) Des Cloizeaux, J. *J. Phys. (Les Ulis, Fr.)* **1975**, *36*, 281.
(34) Daoud, M.; Cotton, J. P.; Farnoux, B.; Jannink, G.; Sarma, G.; Benoît, H.; Duplessix, R.; Picot, C.; de Gennes, P.-G. *Macromolecules* **1975**, *8*, 804.
(35) Candau, F.; Strazielle, S.; Benoît, H. *Eur. Polym. J.* **1976**, *12*, 95.
(36) Roots, J.; Nystrom, B. *Polymer* **1979**, *20*, 148.
(37) Noda, I.; Kato, N.; Kitano, T.; Nagasawa, M. *Macromolecules* **1981**, *14*, 668.
(38) Des Cloizeaux, J.; Noda, I. *Macromolecules* **1982**, *15*, 1505.
(39) (a) Adam, M.; Delsanti, M. *J. Phys. (Les Ulis, Fr.)* **1980**, *41*, 713. (b) Wilzius, P.; Haller, H. R.; Cannell, D.; Schaeffer *Phys. Rev. Lett.* **1984**, *53*, 834.
(40) Brown, W. *Macromolecules* **1986**, *19*, 1083.
(41) Brown, W. *Macromolecules* **1985**, *18*, 1713 and references therein.

Diffusion of Polystyrene Solutions through Model Membranes. 2. Experiments with Mixture Solutions

G. Guillot

Physique de la Matière Condensée† Collège de France, 75231 Paris Cedex 05, France.

Received June 27, 1986

ABSTRACT: The diffusion of bimodal solutions of polystyrene molecules through model porous membranes of pore radius R_p = 75 nm has been examined as a function of the polymer concentration and of the solution composition in long and short chains. With mixtures of long and short chains, we have obtained two new results by analyzing the composition of the solutions after passage through the membrane: (1) In a dilute concentration regime, the long chains stay blocked by the membrane, but the short chains experience an expulsion through the membrane; it can be interpreted as an osmotic expulsion due to the retention of the long chains. (2) The transport of the long chains through the membrane is also accelerated when the number of long chains is kept constant and the concentration is increased by the addition of short chains above the overlap concentration of short chains c_m*. This enhanced diffusion may be attributed to the increase of the long-chain partition coefficient in the presence of short chains. The results are in qualitative agreement with a simple virial expansion model where the same parameters are used as in the analysis of single-chain diffusion kinetics.[1]

Introduction

Solute transport in porous media is generally considered to be controlled by the size of the solute as compared to the pore size. This behavior is well corroborated by a variety of experiments as well as theoretically for solutes small compared to the pore size (see ref 1–9 of the accompanying paper[1]). However, long flexible chains have been observed to enter into pores smaller than their hydrodynamic radius when either the concentration[1-5] or the flow rate[6,7] is increased. Simple scaling arguments[8,9] show that in the absence of flow, long flexible chains should

† Unité Associée au CNRS (U.A. 792).

0024-9297/87/2220-2606$01.50/0

enter freely into small pores at high enough concentration: the partition coefficient (ratio of the chain concentration inside the pore to the outside concentration) should be comparable to 1 when interactions between monomers are screened down to distances smaller than the pore size. It is then expected that the partition coefficient of large chains stays low in dilute conditions and increases with concentration.

We recently reported data on the diffusion of large flexible chains through track-etched membranes of well-defined geometry (porosity, thickness, and pore radius) in the absence of flow.[5] The drastic acceleration of diffusion with concentration could be attributed to the increase of the partition coefficient as described from scaling arguments. In the accompanying paper,[1] similar diffusion experiments have been conducted with two molecular weights. The short chains (not strongly excluded from the pores in dilute conditions) have diffusion kinetics moderately dependent on concentration, while the long chains (excluded from the pores in dilute conditions) present a large acceleration of their diffusion kinetics. These concentration effects attributed to the increase of the partition coefficient are also well taken into account by a simple virial expansion approach, using virial coefficients from previous investigations on the same solutions (polystyrene in ethyl acetate).

In the present paper, we examine the dependence of the diffusion kinetics on both the polymer concentration and the solution composition with mixture solutions of the same two molecular weights as in ref 1.

Theoretically, the diffusion kinetics of bimodal solutions are more complex to describe than for single solute solutions: in the presence of three components (two solutes and one solvent), it is necessary to introduce two exchange flows of polymer with solvent, with two coupled forces. Even with noninteracting solutes, one expects semiequilibrium situations to appear if the membrane permeability differs appreciably between the two solutes.[10] The diffusion kinetics is also changed, although this effect stays negligible at low solute volume fractions.[10] At higher concentrations and with flexible chains, new effects are also expected. The conformations of flexible chains in bimodal solutions have been recently described:[11] a long dilute chain is shown to partially deswell when short chains are added to the solution, at concentrations higher than the short-chain overlap concentration. The size of the long chain is then decreased as compared to the pore size, which should favor the entrance of the long chain into the pore.

Our results obtained with well-characterized polymers and membranes are also of practical interest: solutions used in applications such as enhanced oil recovery are often fairly polydisperse. A qualitative insight of the effect of polydispersity may be given by experiments conducted with bimodal solutions.

Experimental Section

A. Materials. (1) Membranes. Membrane preparation and characterization have been described elsewhere in more detail.[5,12] Latent tracks are formed in polycarbonate films by heavy ion irradiation (Kr^{25+} ions accelerated at 6 MeV/N) performed in A.L.I.C.E. synchrotron in Orsay. These tracks are later etched by a sodium hydroxide solution to produce cylindrical pores spanning the membrane. The pore density is fixed by the irradiation dose and the pore radius is governed by the duration of the etching.

All the diffusion experiments were conducted with membranes of comparable geometric characteristics: membrane thickness $L = 10\ \mu m$, pore radius $R_p = 75$ nm, and total number of pores $N_p = 8 \times 10^8$ on a surface 1 cm^2. Such a high porosity p (p = 14%) was chosen to shorten the duration of the diffusion experiments. It was easily checked that no macroscopic tearing had occurred on either membrane through the order of magnitude of the times characterizing the diffusion of the polymer molecules.

It has been checked that the solvent chosen, ethyl acetate, does not alter the membrane properties and that there is no adsorption of polymer on the membranes.[5]

(2) Solutions. We have prepared by weighing polystyrene solutions of the two molecular weights $M_w = 6.77 \times 10^6$ and $m_w = 8.7 \times 10^5$ in freshly distilled ethyl acetate. The solutions are prepared in advance and they are allowed to homogenize by gentle intermittent stirring for 2 or 3 weeks prior to a diffusion experiment.

The large molecular weight has the same origin as in ref 5; it is a commercial sample of Toyosoda (grade F-700). Its polydispersity as given by the manufacturer is $I = 1.14$. We have used for the small molecular weight sample polystyrene labeled with spiropyran synthesized by Professor Rempp in Strasbourg. After anionic preparation, the living polymer has been divided into two parts, one was deactivated with methanol to give unlabelled chains, the other was deactivated with a solution of spiropyran molecules to give polystyrene chains with one spiropyran molecule at each extremity.[13] Labeled and unlabeled chains of this polystyrene have been characterized by gel permeation chromatography.[14] The unlabeled chain molecular weight is 6.2×10^5 and their polydispersity index 1.2. The labeled chain distribution is much broader, and presents two maxima at 6×10^5 and 1.2×10^6; this bimodal distribution is probably due to duplications that occurred during the spiropyran labeling process. The weight-average molecular weight of the labeled chains is then larger: $m_w = 8.7 \times 10^5$ and their polydispersity index $I = 1.4$.

The hydrodynamic radius of the chains has been determined by quasi-elastic light scattering performed in dilute conditions:[5] $R_H = 58 \pm 3$ nm for the long chains and $r_H = 24 \pm 2$ nm for the short chains. We have also observed that for large chains ($M_w > 10^6$), the scaling law $R_H \propto M_w^{0.55\pm0.02}$ characteristic of good solvent conditions is followed.

The mixture solutions are characterized by the total monomer concentration c (expressed in g/g) and by the proportion of long chain monomers in the mixture X. The monomer concentrations for long (N) and short (n) chains are obtained by respectively $c_N = Xc$ and $c_n = (1 - X)c$. The concentrations in N and n chains are prepared to a 2% accuracy, which fixes the accuracy on X to 5%.

(3) Diffusion Cell. We have used the same diffusion cell as in ref 1 and 5, where it is described in more details. A porous membrane of 1-cm^2 area separates two compartments of respective volumes V_1 and V_2. V_1 and V_2 are measured by weighing to a 1% accuracy during the filling of the cell. Typically, $V_1 = 0.8$ cm^3 and $V_2 = 3.2$ cm^3. Both compartments are tightly sealed to prevent solvent evaporation. Compartment 2 is equipped with two quartz windows which permit optical density measurements.

B. Methods. (1) Spectroscopy. The kinetics of diffusion are followed by absorption spectroscopy. All measurements are done on a spectrophotometer Varian Cary 219 in the double-beam automatic-gain mode.

The total polystyrene concentration in compartment 2, c_2, is monitored from the absorption of styrene at 268 nm. Because of the long optical path of the cell (2 cm), the upper limit to an in situ measurement of c_2 is 10^{-3} g/g, corresponding to an optical density of 3.

The labeled chain concentration in compartment 2 can be detected from the presence of the spiropyrans. The spiropyran absorption shoulder at 335 nm is not distinguishable in the broad scattering spectrum of polystyrene, but spiropyran also exhibits an absorption band (λ_{max} = 580 nm in ethyl acetate) after ultraviolet excitation. This absorption signal is measured after illumination for 1 s of the solutions by the light of a 200-W mercury lamp collimated and filtered around 350 nm. However, the precision of this measurement is poor, 10–20%, and the signal may decrease, typically by 50% after 40–50 h, presumably because of a progressive bleaching of the chromophores.

It is then necessary to use a complementary technique to analyze the composition of the solutions on the time scale of a diffusion experiment (4–10 days).

(2) Sedimentation. We have analyzed the composition of the solutions by sedimentation areas, using a Spinco Model E

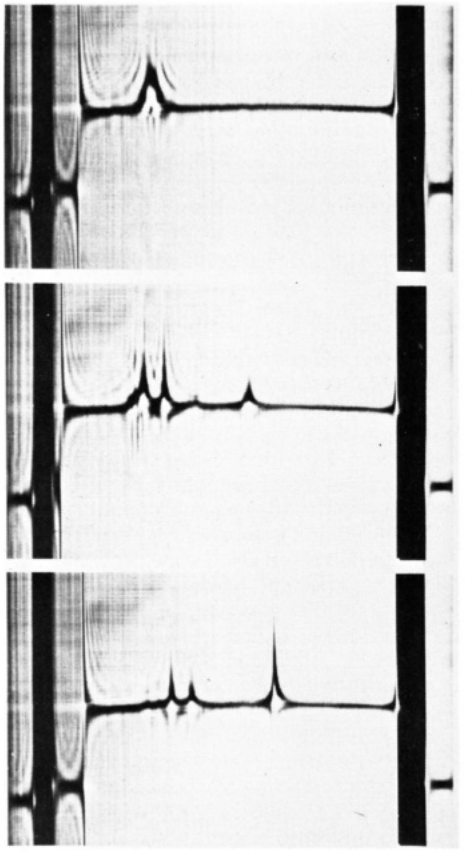

Figure 1. Concentration gradient profiles observed by a Schlieren optical system during the ultracentrifuge runs performed with solutions of total polystyrene concentrations 5×10^{-4} g/g and of various long chain proportions X. From top to bottom: (a) $X = 0$; (b) $X = 0.2$; (c) $X = 0.5$.

Beckman analytical ultracentrifuge, in conjunction with a Schieren optical system.

The solutions are diluted to fixed concentrations by weighing and left for some days to reach equilibrium. After control of their concentration by optical density measurements, they are transferred to an ultracentrifuge cell (13-mm optical path, 4° single sector). The cells are accelerated to 30 000 rpm in 15 ± 1 min. The concentration gradient profiles are recorded on photographic plates at comparable intervals of time after the desired speed has been reached. During all the runs, the temperature of the rotor is regulated at 25 ± 0.1 °C by a RTIC unit. After the runs, the recorded pictures are enlarged by a factor of 10 on photographic paper to measure the positions of the concentration gradient profile peaks and their areas.

We have calibrated the analysis of molecular weight distribution by examining the concentration gradient profiles of solutions of known composition at a total polystyrene concentration $c = 5 \times 10^{-4}$ g/g.

The broad profile obtained with the solution of low molecular weight alone ($X = 0$) (Figure 1a) reflects the large polydispersity of this sample noted in GPC analysis. Two peaks can be followed during the run. The data are represented in Figure 2 in a diagram of $\ln (1 + d/d_m)$ vs. elapsed time, where d and d_m are the distances between respectively the meniscus and the peak, and the center of rotation and the meniscus. The straight lines in Figure 2 correspond to the sedimentation coefficients of the two peaks, respectively slow and rapid: $s_{slow} = (1.20 \pm 0.03) \times 10^{-12}$ s and $s_{rapid} = (1.37 \pm 0.04) \times 10^{-12}$ s.

The profiles of mixture solutions have been also recorded. In Figure 1, parts b and c show respectively typical profiles for the compositions $X = 0.20$ and 0.50. At small distances of the meniscus, a wide profile with two peaks again reflects the broad distribution of the low molecular weight species; a more rapid fine peak is also observed. The data corresponding to these peaks are reported in Figure 2. The slowest peak lies between the two peaks obtained with the low molecular weight species alone. The

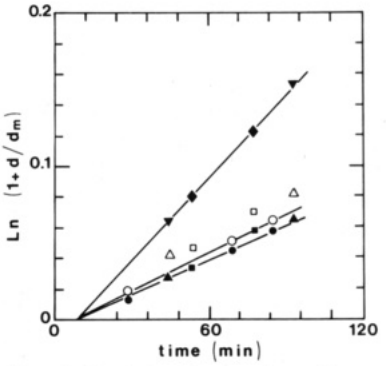

Figure 2. Sedimentation boundary peak position versus elapsed time for solutions of total polystyrene concentration 5×10^{-4} g/g and of long chain proportion X on a semilog scale. A broad profile with two peaks is observed for all compositions: $X = 0$ (●, ○); $X = 0.2$ (▲, △); $X = 0.5$ (■, □). Full symbols refer to the peak closer to the meniscus, open symbols to the other peak. A third fine rapid peak is also observed for $X = 0.2$ (▼) and $X = 0.5$ (◆). The lines correspond to sedimentation coefficients s_{slow}, s_{rapid}, and S as explained in the text.

intermediate peak is much farther from the meniscus than the data corresponding to the sedimentation coefficient s_{rapid}, and the points do not align with the same origin as the other peaks. The fine rapid peak corresponds to a sedimentation coefficient $S = (2.9 \pm 0.1) \times 10^{-12}$ s for both compositions $X = 0.20$ and 0.50.

The sedimentation coefficients deduced of Figure 2 can be compared to values from the literature obtained for polystyrene in ethyl acetate. Taking into account the molecular weight dependence, we can estimate from Vidakovic's data[15] the sedimentation coefficients of different molecular weights taken alone at a concentration 5×10^{-4} g/g. We obtain for chains of molecular weight 6×10^5, 1.2×10^6, and 6.77×10^6 sedimentation coefficients of respectively $(1.1 \pm 0.05) \times 10^{-12}$, $(1.4 \pm 0.05) \times 10^{-12}$, and $(2.9 \pm 0.1) \times 10^{-12}$ s, in excellent agreement with the values respectively s_{slow}, s_{rapid}, and S. Therefore, the two peaks observed in the sedimentation profile of labeled polystyrene alone ($X = 0$) closely correspond to the two maxima of the molecular weight distribution of this sample. In the two profiles for $X = 0.20$ and 0.50, the fine rapid peak can be identified as the sedimenting boundary of the 6.77×10^6 molecular weight species, but the two other peaks are more rapid than expected and cannot be easily identified with a sedimenting boundary.

An explanation for the anomalous behavior of the two slow peaks of the profiles obtained for $X = 0.20$ and 0.50 can be qualitatively advanced. As the runs proceed, the slow component of the mixture gets more and more separated from the fast one. Since the sedimentation coefficient increases as concentration decreases, this could explain a progressive acceleration of the sedimentation rate of the slow component, analogous to the self-sharpening of boundaries.[16,17]

From a measurement of the areas under the peaks, the rapid peak relative area A can be deduced and compared to X, proportion of high molecular weight monomers in the mixture solutions: $A = 0.27 \pm 0.04$ for $X = 0.20 \pm 0.01$; $A = 0.50 \pm 0.04$ for $X = 0.50 \pm 0.03$.

The comparison shows that the rapid peak area closely reflects the quantity of large-chain monomers. Therefore the measurements of A gives a good evaluation of the composition of the solution, with the restriction that the accuracy gets poorer for smaller X. Since X could be lower than 0.10 in the solutions to be analyzed, a higher polystyrene concentration was chosen than in the calibration runs (10^{-3} g/g instead of 5×10^{-4} g/g). The profiles recorded at this concentration present the same trends. The peak corresponding to the large sedimentation coefficient S can be easily observed for X as low as 0.05.

C. Description of a Diffusion Experiment. Both compartments of the diffusion cell are first carefully rinsed several times with filtered, freshly distilled solvent. Compartment 1 is then filled with a polymer solution at the initial total polystyrene concentration $c_{1,0}$ and of large-chain proportion $X_{1,0}$, while compartment 2 is filled with pure solvent. Both compartments are completely filled to ensure constant-volume conditions. Under

Table I
Results of Mixture Experiments

	experiment code letter				
	A	B	C	D	E
$c_{1,0}$, g/g	10^{-2}	2×10^{-2}	2.5×10^{-2}	4.5×10^{-2}	4.5×10^{-2}
$X_{1,0}$, %	50	50	20	11.1	11.1
$\mathcal{R}$, h/cm	$\mathcal{R}' = 53 \pm 4$,[a] $\mathcal{R}'' = (1.1 \pm 0.3)\ 10^3$	44 ± 4	51 ± 6	53 ± 4	47 ± 4
t_{int}, h	528	240	100	120	120
c_1, g/g	$(3.5 \pm 0.05) \times 10^{-3}$	$(4.7 \pm 0.1) \times 10^{-3}$	$(8.1 \pm 0.1) \times 10^{-3}$	$(1.32 \pm 0.02) \times 10^{-2}$	$(1.18 \pm 0.02) \times 10^{-2}$
X_1, %	83 ± 2	49 ± 2	30 ± 2	10 ± 2	24 ± 2
c_2, g/g	$(1.6 \pm 0.05) \times 10^{-3}$	$(4 \pm 0.05) \times 10^{-3}$	$(4.2 \pm 0.05) \times 10^{-3}$	$(7.8 \pm 0.1) \times 10^{-3}$	$(7.2 \pm 0.1) \times 10^{-3}$
X_2, %	39 ± 2	48 ± 2	4 ± 2	12 ± 2	12 ± 3
c_{n1}/c_{neq}, %	60 ± 10				
c_{n2}/c_{neq}, %	100 ± 10	100 ± 10	100 ± 10	90 ± 10	80 ± 10
c_{N2}/c_{Neq}, %	65 ± 10	90 ± 5	20 ± 12	100 ± 20	85 ± 20
$\mathcal{R}_N$, h/cm	810 ± 220	150 ± 30	300 ± 110	<120	<190

[a] $\mathcal{R}'$ corresponds to τ' and $\mathcal{R}''$ to τ'' in Figure 3.

the concentration difference established across the membrane, the polymer chains tend to diffuse, and the total polystyrene concentrations c_1 and c_2 of both compartments evolve toward the total equilibrium concentration $c_{eq} = c_{1,0}V_1/(V_1 + V_2)$. Each compartment is constantly homogenized by small magnetic stirring bars, at a stirring rate $f = 80 \pm 20$ rpm, in order to get well-defined limiting conditions for the diffusion. $c_{1,0}$ is determined by absorption spectroscopy at 268 nm in a quartz cuvette of 1-mm optical path to a relative accuracy of ±1.5%. c_2 is monitored as a function of time by spectroscopy until $c_2 > 10^{-3}$ g/g. The short-chain concentrations in compartment 2 can be also evaluated during the first 24–30 h of the experiment by the photoexcited spectrum of spiropyran.

After 4–10 days, the experiment is interrupted. c_1 and c_2 are determined by transferring the solutions in a quartz cuvette of 1-mm optical path and measuring their absorption at 268 nm. The mixture solutions are diluted to a total polystyrene concentration 10^{-3} g/g a few days in advance to the sedimentation runs. The long-chain proportions at interruption X_1 and X_2 respectively for compartments 1 and 2 are determined by the sedimentation area measurement.

In some cases, successive experiments have been undertaken with the same membrane; the cell was thoroughly rinsed several times after interruption. All the experiments have been performed at room temperature $T \simeq 20$ °C.

Results

The evolution of concentrations in compartment 2 gives access to the diffusion coefficients through the membrane. If both types of chains stay dilute inside the pore, each exchange flow of polymer with solvent proceeds at a rate almost independent of the other chains. We may then define the diffusion resistance $\mathcal{R}$ as the ratio of the concentration difference between the two compartments of the flux of molecules for each type of chain, independently of the presence of the others. $\mathcal{R}_n$ (diffusion resistance of n chains) and $\mathcal{R}_N$ (diffusion resistance of N chains) are related to the corresponding diffusion rates τ_n^{-1} and τ_N^{-1} by

$$\mathcal{R}_A = \tau_A S \left(\frac{1}{V_1} + \frac{1}{V_2} \right) \qquad \text{where } A = n, N$$

Resistances rather than diffusion rates of the experiments will be compared because comparable membranes of surface S but cells of various volumes V_1, V_2 have been used.

If the boundary condition of uniform concentrations in each compartment is achieved, the resistance to diffusion is only due to the membrane. The membrane resistance gives access to the effective diffusion coefficient through the membrane $D_{eff\,A}$, at known porosity p and membrane thickness L: $\mathcal{R}_A = L/(pD_{eff\,A})$.

We have checked that diffusional boundary layers due to insufficient stirring of the solution are negligible with dilute solutions of the two molecular weights in ref 1, where more quantitative data on the boundary layer effect are presented.

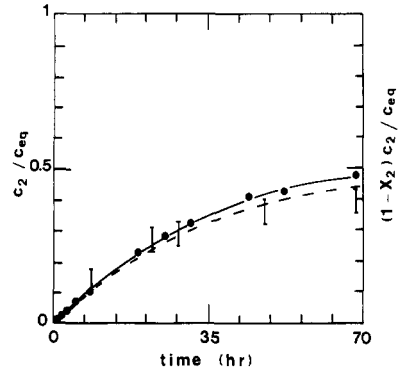

Figure 3. Total polystyrene concentration in compartment 2 (●) and n chain concentration in compartment 2 $(1 - X_2)c_2$ (error bars), both normalized to the *total* polystyrene concentration at equilibrium c_{eq}, for experiment A ($c_{1,0} = 10^{-2}$ g/g, $X_{1,0} = 50\%$). Both proportions follow similar kinetics for $t < 35$ h; the n chain concentration evolutes slower later. The dashed line represents a simple diffusion process: $c_2/c_{eq} = {}^1/_2(1 - e^{-t/\tau})$ and the full line the sum of two independent diffusion processes: $c_2/c_{eq} = {}^1/_2(1 - e^{-t/\tau'}) + {}^1/_2(1 - e^{-t/\tau''})$. The corresponding resistances $\mathcal{R}'$ and $\mathcal{R}''$ are reported in Table I.

The initial concentration $c_{1,0}$ and the initial N chain proportion $X_{1,0}$ are reported in Table I for the diffusion experiments performed with mixture solutions. Each experiment is designated by a code letter (A–E) as indicated in Table I.

A. Diffusion Kinetics. (1) Total Polystyrene Concentration. The evolution with time of c_2, total polystyrene concentration in compartment 2, is reported in Figure 3 for A, performed with equal initial concentrations in N and n chains: $(1 - X_{1,0})c_{1,0} = X_{1,0}c_{1,0} = 5 \times 10^{-3}$ g/g. At short times ($t < 8$ h), the normalized total polystyrene concentration c_2/c_{eq} follows an exponential law:

$$c_2/c_{eq} = {}^1/_2(1 - e^{-t/\tau_{eff}})$$

with $\tau_{eff} = 34 \pm 1$ h (dashed line in Figure 3). At longer times, the kinetics are more rapid than this single exponential. A sum of two half-exponential laws better describes the whole kinetics (full line in Figure 3)

$$c_2/c_{eq} = {}^1/_2(1 - e^{-t/\tau'}) + {}^1/_2(1 - e^{-t/\tau''})$$

with $\tau' = 34 \pm 1$ h and $\tau'' = 700 \pm 150$ h. The times τ' and τ'' correspond to resistances $\mathcal{R}' = 53 \pm 4$ h/cm and $\mathcal{R}'' = (1.1 \pm 0.3) \times 10^3$ h/cm, respectively, comparable to those characteristic of the diffusion kinetics of the n and N

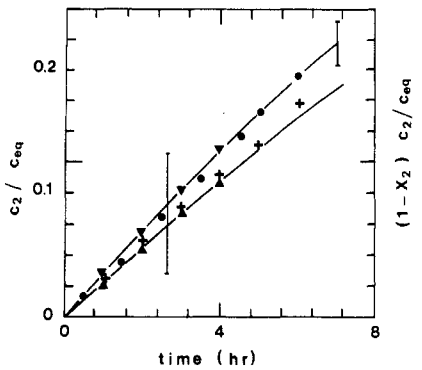

Figure 4. Same as in Figure 3: c_2/c_{eq} is shown for mixture experiments B (●), C (+), D (▲), and E (▼). Only early kinetics ($t < 8$ h) are reported (c_2/c_{eq} (25%)), because of the upper limit to the measurement of c_2. The n chains data are indicated by error bars. They follow similar kinetics as the total polystyrene concentration on this time scale.

chains, respectively, alone at an initial concentration of 5×10^{-3} g/g.[1]

Figure 4 presents c_2/c_{eq} for all the other mixture experiments, at the short time scale when c_2 can be followed: the kinetics of c_2/c_{eq} are similar for all these experiments for $t < 8$ h. Exponential laws, $c_2/c_{eq} = (1 - e^{-t/\tau_{eff}})$, have been force fitted onto the data. For $c_{1,0} < 2.5 \times 10^{-2}$ g/g, they are comparable to those obtained with n chains alone.[1] The two experiments D and E performed at $c_{1,0} = 4.5 \times 10^{-2}$ g/g and $X_{1,0} = 11.1\%$ give values of $\mathcal{R}$ reproducible one with the other within 10%, but larger by 20% than for n chains alone at a comparable concentration.[1] The 20% difference noticeable in Figure 4 between D and E is mainly due to the volume differences between the two different cells used in these experiments.

(2) n Chain Concentration. The n chain concentration in compartment 2 $(1 - X_2)c_2$ has been estimated from the absorption spectrum of photoexcited spiropyran. The data corresponding to A are reported in Figure 3. For $t < 35$ h, c_2/c_{eq} and $(1 - X_2)c_2/c_{eq}$ have comparable values; this indicates that the proportion of N chains in compartment 2, X_2, is low: very few N chains have crossed the membrane in this time scale. At longer times, the n chain concentration seems to evolve slower, but this may be due to partial bleaching of the chromophores.

In Figure 4 $(1 - X_2)c_2/c_{eq}$ for B also indicates that $X_2 \simeq 0$ at short times ($t < 8$ h). Comparable values of $(1 - X_2)c_2/c_{eq}$ have been obtained for the other mixture experiments, C–E, where the initial proportion of N chains is lower: $X_{1,0} = 20\%$ and $X_{1,0} = 11.1\%$; however, the large error bars in Figures 3 and 4 give evidence that the poor relative accuracy of the determination of the n chain quantity does not enable to estimate X_2. At longer times ($t > 30$ h), the decrease of the absorption of photoexcited spiropyran which was observed in some check samples shows that the kinetics of the n chains cannot be correctly followed.

B. Sedimentation Results. The total polystyrene concentration c_i and the N chain proportion X_i determined in each compartment $i = 1,2$ after interruption at t_{int} are reported in Table I. It can be checked that these results respect the conservation of the quantity of both types of polymer molecules present at the beginning of the experiment, taking into account the accuracy of the determination of $c_{1,0}$, $X_{1,0}$, c_i, X_i, and V_i. The concentrations in each compartment $i = 1,2$ can be deduced, for the n chains, by $c_{ni} = (1 - X_i)c_i$ and for the N chains by $C_{Ni} = X_i c_i$.

Information on the kinetics of diffusion is given by the ratios $c_{n2}/c_{neq} = (1 - X_2)c_2/(1 - X_{1,0})c_{1,0}[(V_1 + V_2)/V_1]$ for the n chains and $c_{N2}/c_{Neq} = X_2 c_2/X_{1,0}c_{1,0}[(V_1 + V_2)/V_1]$ for the N chains reported in Table I. For all the experiments, c_{n2} is close to c_{neq}, equilibrium concentration of the n chains: their diffusion has proceeded on time scales shorter than t_{int}. On the other hand, c_{N2} stays smaller than c_{Neq}, equilibrium concentration of the N chains after an elapsed time t_{int}, in some experiments: the diffusion of the N chains is then hindered. For a more quantitative comparison, we have calculated the diffusion rate τ_N^{-1} of the N chains, assuming that the evolution of c_{N2} has proceeded toward c_{Neq} at an exponential rate: $c_{N2}/c_{Neq} = (1 - e^{-t/\tau_N})$. The corresponding resistances $\mathcal{R}_N$ are reported in Table I.

Three important results have been obtained:

(1) Slow Diffusion of the N Chains. The resistance to diffusion of the N chains in A is evaluated to be $\mathcal{R}_N = 810 \pm 220$ h/cm, of the same order of magnitude as the resistance $\mathcal{R}''$ corresponding to the slow time τ'' in Figure 3. This result confirms that the kinetics of the total polystyrene concentration in Figure 3 can be approximated as the sum of two independent processes, the diffusion of the n chains and of the N chains. The N chains diffuse 20 times slower than the n ones. The value of $\mathcal{R}_N$ is also in excellent agreement with the value obtained for N chains alone at $c_{1,0} = 4.85 \times 10^{-3}$ g/g: $\mathcal{R} = 10^3$ h/cm in ref 1. Therefore, the N chain diffusion stays slow in the mixture solution $c_{1,0} = 10^{-2}$ g/g, $X_{1,0} = 0.5$, as slow as for N chains alone at the same concentration.

(2) Expulsion of the n Chains. We may note that in A $c_{n2} = (1 \pm 0.05) \times 10^{-3}$ g/g is higher than $c_{n1} = (6 \pm 0.8) \times 10^{-4}$ g/g. At $t_{int} = 528$ h, the n chains have been expelled from compartment 1 to compartment 2, while the majority of the N chains have stayed in compartment 1. The expulsion can be also characterized by the ratios c_{n2}/c_{neq} and c_{n1}/c_{neq} reported in Table I.

(3) Acceleration of the Diffusion of the N Chains. B has been performed with initial concentrations twice as high as those of A. The resistance to diffusion of the N chains decreases between A and B by a factor 5, in agreement with the dependence of $\mathcal{R}$ on $c_{1,0}$ observed for N chains alone with membranes of comparable porosity (see ref 1). The value of $\mathcal{R}_N$ thus obtained also corresponds to a negligible proportion of N chains in compartment 2 during the first hours of the experiment, in agreement with the data of Figure 4.

In C, the initial N chain concentration $X_{1,0}c_{1,0}$ is kept at 5×10^{-3} g/g as in A, while the initial n chain concentration $(1 - X_{1,0})c_{1,0}$ is increased at 2×10^{-2} g/g. From the estimated resistances $\mathcal{R}_N$, the diffusion of the N chains is more rapid by a factor 2.5 than in A. This acceleration is, however, much less than for N chains alone:[1] the resistance decreases by a factor 10 between $c_{1,0} = 4.85 \times 10^{-3}$ g/g and 2×10^{-2} g/g.

D and E are similar to C, except for $(1 - X_{1,0})c_{1,0} = 4 \times 10^{-2}$ g/g. At $t_{int} = 120$ h, c_{N2} is close to c_{Neq}: the N chains have almost equilibrated their concentrations on both sides of the membrane. Although only a higher limit can be given for $\mathcal{R}_N$, we observe from Figure 6 a marked acceleration of the diffusion of the N chains, over a factor 8, when their initial concentration is kept at 5×10^{-3} g/g and the initial concentration in n chains is increased from 5×10^{-3} g/g (A) to 4×10^{-2} g/g (D and E).

Discussion

The presence of chains of another species added to a monodisperse solution may provoke semiequilibrium situations. It can also change the diffusion kinetics.

The only definite equilibrium situation is of course attained at equal concentrations in the two compartments,

for both types of chains. But semiequilibrium may also exist if there is an appreciable difference in the permeability of the membrane between the two species:[10] the smaller solute is expelled at short time scales when the larger one stays blocked by the membrane. The semiequilibrium situation is defined by the equality of the chemical potentials of solvent and of the small solute in the two compartments.

In presence of two solutes, it is necessary to introduce two exchange flows of each solute with solvent to describe the diffusion kinetics. Each flow should depend linearly not only on the corresponding force, the chemical potential gradient of its own species, but also on that the other one. However, the acceleration of the diffusion kinetics of one species by another should stay a second-order effect in dilute regimes:[10] if both types of chains stay dilute once they have entered the pore, their diffusion kinetics inside the pore should proceed independently. On the other hand, the partition coefficient of one type of chain from the pore may be influenced by the presence of other chains, especially in concentration regimes close to a semidilute regime. For comparison with our results, we first classify the experiments by their concentration regimes. Then we examine theoretically the dependence of the partition coefficients for both types of chains in the presence of one another. Last we compare these predictions to the results.

A. Concentration Regimes. The mixture experiments may be classified by comparing the initial concentrations in N and n chains to the corresponding first overlap concentrations. We choose the values which appear relevant to the case of single species: $c^*_M = 5 \times 10^{-3}$ g/g and $c^*_m = 3 \times 10^{-2}$ g/g. We consider with such a choice that the N chains are kept at the limit of their dilute regime in A, C, D, and E, while the n chains stay dilute in A and C and begins to be semidilute in D and E. Similarly, in B the N chains are initially in a semidilute regime and the n chains in a dilute one.

B. Theoretical Position of the Problem for N Dilute Chains. When n chains are added to a dilute solution of N chains, two effects may increase the partition coefficient of the N chain from the pores: the presence of the n chains may change the configuration of the N chains and partially deswell them; besides it also increases their osmotic potential, both inside and outside the pore.

(1) Deswelling of the N Chains in Presence of the n Chains. Joanny et al.[11] have constructed the phase diagram of a bimodal solution in an athermal solvent starting from the Flory description[18] of one long chain in a melt of shorter chains. They have shown that the presence of short (n) chains reduces the solvent quality experienced by the long (N) chains, through an excluded volume parameter function of the volume fraction ϕ_n of the n chain monomers in the solution ($\phi_n \propto c_n$). They have in particular deduced the size R of one dilute N chain in the solution as a function of ϕ_n. For $\phi_n < \phi^*_m = n^{-4/5}(\phi^*_m \propto c^*_m)$, the conformation of the N chain is only slightly changed as compared to its conformation in pure solvent:

$$R(c_n) = R(c_n=0)(1 + c_n/c^*_m)^{-1/5} \simeq R(c_n=0)$$

For $c_n > c^*_m$, the N chain stays swollen, but R decreases with c_n:

$$R(c_n) = R(c_n=0)[1 + (c_n/c^*_m)^{5/4}]^{-1/5} \simeq R(c_n=0)(c_n/c^*_m)^{-1/4}$$

The volume fraction $\phi_m{}^+$ upper limit of this swollen regime is

$$\phi_m{}^+ = \phi^*_m(N/n)^{4/5} = N^{4/5}n^{-8/5}$$

Since ϕ_n must stay less than 1, $\phi_n{}^+$ only exists when $n > N^{1/2}$. Under this condition, the conformation of the N chain becomes ideal[19] for $c_n > c_m{}^+$. Following these scaling arguments, we may expect that the confinement potential of one N chain in dilute solution[20] $\mu_{\text{conf}\,N} = k_BT\,(R/R_p)^{5/3}$ is lowered in presence of a concentration c_n of n chains inside the pore and becomes, for $c_n < c^*_m$,

$$\mu_{\text{conf}\,N}(c_n) = \mu_{\text{conf}\,N}(c_n=0)(1 + c_n/c^*_m)^{-1/3}$$

for $c^*_m < c_n < c_m{}^+$,

$$\mu_{\text{conf}\,N}(c_n) = \mu_{\text{conf}\,N}(c_n=0)[1 + (c_n/c^*_m)^{5/4}]^{-1/3}$$

The regime where the N chains stay dilute but where their conformation should become ideal[19] has not been investigated: the n chains concentration $c_m{}^+ = c^*_m \times 6$ is so high that the methods which we have used would not be able to detect the too low proportion of N chains monomers in the solutions.

(2) Osmotic Potentials. In a concentration regime where both types of chains stay isolated ($c_n < c^*_m$ and $c_N < c^*_M$), the osmotic pressure of a heterogeneous polymer solution can be described by a virial expansion. The first interaction term is of the form[21,22]

$$\Delta\pi/RT\rho^2 = A_{2_{n,n}}c_n{}^2 + A_{2_{N,N}}c_N{}^2 + 2A_{2_{n,N}}c_nc_N$$

where c_n (c_N) is the concentration of n (N) chains in weight/weight and $A_{2_{i,j}}$ the virial coefficient proportional to the mutual excluded volume v_{ij} of one i chain by one j chain. For $i = j$, we recover the usual virial coefficient of the corresponding monodisperse case. The cross-coefficient $A_{2_{n,N}}$ has been theoretically shown to be of the same order of magnitude as the virial coefficient $A_{2_{n,n}}$ of the lower molecular weight compound.[21,22] Only two coefficients $\alpha_n = 2A_{2_{n,n}}m\rho = 2A_{2_{N,n}}m\rho$ and $\alpha_N = 2A_{2_{N,N}}m\rho$ may be kept and the osmotic potentials $\mu_{\text{os}\,n(N)}$ of the n (N) chains are obtained:

$$\mu_{\text{os}\,n} = k_BTn\alpha_n(c_n + c_N)$$

$$\mu_{\text{os}\,N} = k_BTN(\alpha_Nc_N + \alpha_nc_n)$$

When the N chains are kept dilute at $c_N < c^*_M$, a semidilute regime is attained by adding n chains when $c_n > c^*_m$. The osmotic pressure should be determined by the local monomer concentration, $\Delta\pi\alpha(c_n + c_N)^{9/4}$, and the osmotic potentials be then of the form

$$\mu_{\text{os}\,n} = k_BTk_1\left(\frac{c_n + c_N}{c^*_m}\right)^{5/4}$$

$$\mu_{\text{os}\,N} = k_BTk_1\left(\frac{c_n + c_N}{c^*_M}\right)^{5/4}$$

where $c_n \gg c_N$ and where k_1 is a numerical constant. One may expect k_1 to be the same as for a monodisperse semidilute solution,[1] $k_1 = 2.7$, but we have no knowledge of experimental checks of this point.

(3) Partition Coefficients. The partition coefficients are determined by coupled equations, since the osmotic potentials depend on the inside and outside concentrations of both species. The confinement potential of the N chain is also a function of the pore concentration in n chains: $c_nK_n(c_n,c_N)$. As a first approximation, we consider that the N chain concentration stays negligible inside the pore in all cases. In the limit where the virial expansion applies, the partition coefficients are obtained from

$$K_n(c_n,c_N) = K_n(0,0)\,\exp[n\alpha_n[c_N + c_n(1 - K_n(c_n,c_N))]]$$

$$K_N(c_n,c_N) = K_N(0,0)\,\exp[-[1 + K_n(c_n,c_N)c_n/c^*_m]^{-1/3} + N\alpha_nc_n[1 - K_n(c_n,c_N)] + N\alpha_Nc_N] \quad (1)$$

The results from the diffusion kinetics of single species[1]

enable evaluation of all parameters in this system. $K_n(0,0)$ and $K_N(0,0)$ are the partition coefficients of n and N chains at infinite dilution. $n\alpha_n$ and $N\alpha_N$ are known from the concentration dependence of the diffusion kinetics of single species. Therefore, we can calculate $K_n(c_n,c_N)$ and deduce $K_N(c_n,c_N)$. A similar system of equations can be derived for the partition coefficients in a regime where the N chains stay dilute ($c_N \leq c^*_M$) and where the n chains are semidilute inside as well as outside the pores. It can be solved in the same way as the virial expansion system (1).

C. Comparison to Experimental Results. (1) Dilute Regime for Both Species ($c_N \leq c^*_M$, $c_n \leq c^*_m$); A. a. Diffusion Kinetics. A good description of the diffusion kinetics of polystyrene in Figure 3 is given by the sum of two independent diffusion processes. The two characteristic resistances are in agreement with those evaluated by sedimentation. It is to be noted that $\mathcal{R}'$ and $\mathcal{R}''$ have been determined with the assumption that the driving force for diffusion of one species along the pore is the concentration difference between the two compartments of the corresponding species (prime for n chains, double prime for N chains). Diffusion proceeds slightly more rapidly than for the corresponding type of chain alone at the same concentration and the same porosity.[1] Therefore, the diffusion kinetics of each type of chains through the membrane appears in this experiment almost independent of the presence of the other chains. Indeed, the partition coefficients given by eq 1 are expected to keep in the low concentration regime values comparable to the single-chain case: $K_n(c_n,c_N=0)$ is known to be comparable to 1; $n\alpha_n c_n$ and $n\alpha_n c_N$ stay small; therefore equations 1 should simplify:

$$K_n(c_n,c_N) \lesssim 1$$

$$K_N(c_n,c_N) \simeq K_N(c_n=0,c_N) \ll 1$$

b. Expulsion of the *n* Chains. We have also observed by sedimentation that the n chain concentration is lower in compartment 1 than in compartment 2 at interruption of A. This expulsion of the n chains has appeared while the majority of the N chains has stayed in compartment 1. This can be understood by considering the membrane as semipermeable and by taking into account the effective repulsive interaction between the chains.

The hypothesis of a semipermeable membrane which allows the n chains to diffuse freely and blocks the N chains in compartment 1 is reasonable. Diffusion through the membrane indeed proceeds much slower for N chains than for n chains in this experiment.

A semiequilibrium situation is obtained through the expulsion of the n chains, which build a concentration gradient of sign opposite to the concentration gradient of the N chains blocked in compartment 1. The repartition of the n chains in this situation is deduced from the equality of their chemical potentials on both sides of the membrane μ_{n1} and μ_{n2}. If the N chain concentration in compartment 2, c_{N2}, is negligible ($c_{N2} \approx 0$), we deduce from $\mu_{n1} = \mu_{n2}$ in the virial expansion limit (low concentration regime)

$$\ln (c_{n1}/c_{n2}) = +n\alpha_n(c_{n2} - c_{n1} - c_{N1}) \qquad (2)$$

c_{n1} and c_{n2} are related to $X_{1,0}$ and $c_{1,0}$ through the conservation of the initial number of n chains:

$$(1 - X_{1,0})c_{1,0}V_1 = c_{n1}V_1 + c_{n2}V_2$$

The two quantities c_{n1}/c_{neq} and c_{n2}/c_{neq} which indicate the deviation from equal n chain concentrations on both sides of the membrane have been calculated to satisfy eq 2 for $V_1 = 0.8$ cm^3 and $V_2 = 3.2$ cm^3. They are reported in Figure 5 as a function of the parameter $\alpha = n\alpha_n(1 - X_{1,0})c_{1,0}$ for various values of $X_{1,0}$. Since the volumes of the two compartments differ by the ratio $V_2/V_1 = 4$, the expulsion of the n chains from compartment 1, c_{n1}/c_{neq}, is more easily measurable than their excess in compartment 2, c_{n2}/c_{neq}, as observed in this experiment: $c_{n1}/c_{neq} = 0.6 \pm 0.1$, whereas $c_{n2}/c_{neq} = 1 \pm 0.1$. The parameter α can be deduced from the experimental evaluation of c_{n1}/c_{neq} and from the curve in Figure 5 corresponding to $X_{1,0} = 50\%$, $\alpha_{exp} = 0.65 \pm 0.25$. It can also be evaluated because $n\alpha_n$ is known from the concentration dependence of the partition coefficient of n chains alone:[1] $(n\alpha_n)^{-1} = 1.5 \times 10^{-2}$ g/g. For an initial concentration of n chains $(1 - X_{1,0})c_{1,0} = 5 \times 10^{-3}$ g/g, we obtain $\alpha = 0.33$, in reasonable agreement with α_{exp}.

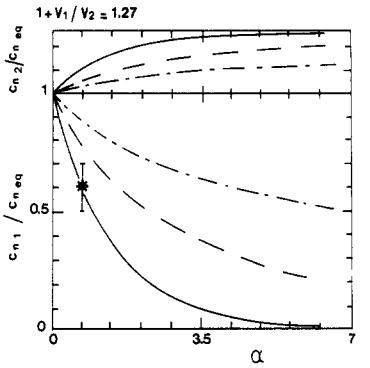

Figure 5. n chain excess in compartment 2 c_{n2}/c_{neq} and expulsion from compartment 1 c_{n1}/c_{neq} calculated from eq 2 in the text as a function of $\alpha = n\alpha_n(1 - X_{1,0})c_{1,0}$ for various values of $X_{1,0}$: full lines $X_{1,0} = 50\%$; dashed lines $X_{1,0} = 30\%$; semidashed lines $X_{1,0} = 20\%$.

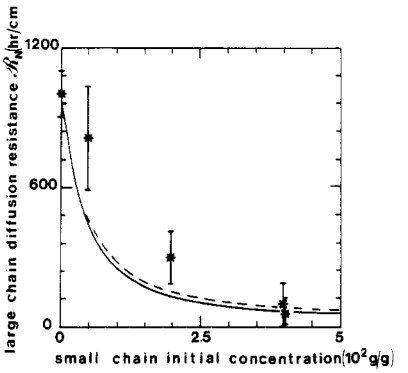

Figure 6. N chain diffusion resistance as a function of n chain initial concentration when the N chains are kept at an initial concentration of 5×10^{-3} g/g. The observed acceleration is quite well taken into account by the N chain partition coefficient K_N calculated as explained in the text: the dashed line corresponds to an increase of K_N in the presence of n chains through an osmotic potential effect, while the full line also includes a confinement effect.

Figure 5 shows that the efficiency of the expulsion, which depends both on $c_{1,0}$ and $X_{1,0}$ (or equivalently α and $X_{1,0}$), should be comparable in A and in C–E and higher in B. It has been observed only in A, since in the other experiments, the N chain diffusion resistance is lowered in higher initial concentrations conditions: the membrane can no longer be considered as semipermeable.

(2) *N* Dilute Regime, Effect of *n* Chain Concentration; A and C–E. $\mathcal{R}_N$ determined by sedimentation is plotted in Figure 6 as a function of the n chain initial concentration $(1 - X_{1,0})c_{1,0}$, for experiments all performed at a N chain initial concentration $X_{1,0}c_{1,0} = 5 \times 10^{-3}$ g/g $= c^*_M$. A marked decrease of $\mathcal{R}_N$ with $(1 - X_{1,0})c_{1,0}$ is observed. Yet it is not as drastic as the decrease of $\mathcal{R}_N$

for N chains alone at their initial concentration.[1] Theoretical curves deduced of eq 1 are also represented in Figure 6. We have used the first part of eq 1 to calculate $K_n(c_n,c_N=5\times10^{-3}\,g/g)$, taking for the parameters the values deduced of the analysis of the single-chain diffusion kinetics:[1] $K_n(c_n=0,c_N=0) = 0.5$ and $(n\alpha_n)^{-1} = 1.5\times10^{-2}$ g/g. The variation of $\mathcal{R}_N$ with $c_n = (1 - X_{1,0})c_{1,0}$ when $c_N = X_{1,0}c_{1,0}$ is kept constant at 5×10^{-3} g/g is obtained from the second part of eq 1 after injection of the calculated K_n. The full line in Figure 6 represents $\mathcal{R}_N(c_n,c_N=5\times10^{-3}\,g/g)$ calculated from

$$\mathcal{R}_N(c_n,c_N=5\times10^{-3}\,g/g) = \mathcal{R}_N(c_n=0,c_N=5\times10^{-3}\,g/g)F_{conf}F_{os}$$

where F_{conf} and F_{os} are respectively the factors which cause the decrease of $\mathcal{R}_N$ through the change in the confinement potential of one N chain and the change in its osmotic potential due to the presence of the n chains:

$$F_{conf} = \exp[(1 + K_nc_n/c^*_m)^{-1/3} - 1]$$

$$F_{os} = \exp[-N\alpha_nc_n(1 - K_n)]$$

The dashed line has been calculated in the same way, but with $F_{conf} = 1$. For both curves, $\mathcal{R}_N(c_n=0,c_N=5\times10^{-3}\,g/g) = 10^3$ h/cm and $(N\alpha_n)^{-1} = (n\alpha_n)^{-1}(1/9.6)$. The two curves are not distinguishable one from the other until $c_n > c^*_m$. From this description, the decrease of $\mathcal{R}_N$ with $(1 - X_{1,0})c_{1,0}$ is mainly due to the osmotic potential factor F_{os}. The theoretical curves deduced from (1) with parameters adjusted from the single-chain diffusion kinetics agree quite well with the data. Yet one should consider that the $\mathcal{R}_N$ data give only higher estimates of the initial resistances $\mathcal{R}_N(c_n,c_N)$. The N chain diffusion kinetics has been assumed to follow a simple exponential law to determine $\mathcal{R}_N$, although one may expect the N chain diffusion to slow down as experiment proceeds for several reasons: (a) we have observed that the diffusion of N chains alone at initial concentrations higher than c^*_M is highly nonexponential and slows down progressively;[1,5] (b) the n chains diffuse more rapidly through the membrane than the N chains, and the decrease of their concentration in compartment 1 during the experiment should also decrease K_N. The good quantitative agreement between our data and eq 1 is probably mainly due to the high value of K_n or to the small concentration difference in n chains between the inside and the outside of the pores.

We may then interpret again the acceleration of the N chain diffusion in the presence of n chains as due to an increase of their partition coefficient from the pores. Its variation is smoother than when the N chain concentration alone is increased, because of the high value of $K_n \lesssim 1$.

(3) N Semidilute, n Dilute Regime ($c_N > c^*_M$, $c_n < c^*_m$); B. a. n Chain Diffusion Kinetics. The resistance $\mathcal{R}$ reported in Table I for B characterizes the early diffusion kinetics ($t < 8$ h) of the total polystyrene concentration c_2 in compartment 2. An equivalent resistance has been obtained with n chains alone at a comparable total initial concentration ($c_{1,0} = 2\times10^{-2}$ g/g).[1] For both experiments, $\mathcal{R}$ has been calculated with the assumption that the driving force for diffusion is the total polystyrene concentration c_1 in compartment 1. This holds for n chains alone, but it should be necessary to introduce two concentration differences in a mixture experiment since two solutes are present. The comparison of c_2 and $(1 - X_2)c_2$ (n chain concentration in compartment B) in Figure 4 also shows that almost only n chains are diffusing on the short time scale $t < 8$ h of B. If this n chain flow is only induced by the n chain concentration difference between the two compartments, the n chain diffusion is then in fact accelerated by a factor of 2 as compared to the n chain only experiment at $c_{1,0} = 2\times10^{-2}$ g/g. We can partly attribute this acceleration to an increase of the n chains partition coefficient K_n. However, K_n changes only by a factor 1.4 between the n chain only experiment, $K_n(c_n=2\times10^{-2}\,g/g,c_N=0) = 0.72$, and B, $K_n(c_n=10^{-2}\,g/g,c_N=10^{-2}\,g/g) = 0.98$, when K_n is calculated from the first part of eq 1 with $K_n(0,0) = 0.5$ and $(n\alpha_n)^{-1} = 1.5\times10^{-2}$ g/g. We do not think that this reflects the limit of the virial approach, since a comparable change in K_n is obtained with a scaling approach. It seems to us that the residual acceleration effect should rather be taken into account by the other driving force due to the N chain concentration gradient along the pore: indeed, for $c_N > c^*_M$, the N chain concentration inside the pore may become of importance.[1,5]

b. N Chain Diffusion Kinetics. Sedimentation shows that in B an equilibrium situation is almost attained for both types of chains at interruption. The resistance characteristic of the N chain diffusion is at least 5 times lower than that in A. We note that the $\mathcal{R}_N$ value reported in Table I gives again only a higher estimate for the initial resistance $\mathcal{R}_N(c_{1,0},X_{1,0})$: it has been calculated with the assumption that the N chains diffuse with a simple exponential law. But the N chain diffusion kinetics may be expected to be progressively slowing down as in the case of N chains alone at concentrations higher than c^*_M.[1,5]

We may evaluate the N chain diffusion resistance $\mathcal{R}_N(c_n,c_N)$ by considering that the n chain initial concentration is too low to change their behavior ($c_n/c^*_m < 1$ and $K_n \simeq 1$). In an analogous way to the analysis of ref 1, the partition coefficient increase or the resistance decrease with initial concentration may be described by using a virial expansion approach (see eq 12 of ref 1),

$$\mathcal{R}_N(c_n\simeq0,c_N) = \mathcal{R}_N(c_n\simeq0,c_N=0)\exp\left[-\frac{c_{N1}(t=0)}{c_V}\right] \quad (3)$$

with $c_V = 2.5\times10^{-3}$ g/g, or by using a scaling approach (see eq 10 of ref 1),

$$\mathcal{R}_N(c_n\simeq0,c_N) = \mathcal{R}_N(c_n\simeq0,c_N=0)\exp\left[-\frac{c_{N1}(t=0)}{c_A}\right]^{5/4} \quad (4)$$

with $c_A = 4.5\times10^{-3}$ g/g. The two approaches can be compared to experiment by calculating the ratio $y = \mathcal{R}_{N(A)}/\mathcal{R}_{N(B)}$ of the N chain resistance to diffusion in A to its value in B. y as evaluated by the sedimentation results $y_{exp} \geq 5$ is in fair agreement with both models: $y = 7.5$ from the virial expansion law (3) and $y = 4.8$ from the scaling appoach (4). We may then consider that the N chain diffusion proceeds as if they were alone in the regime: $c_N > c^*_M$, $c_n < c^*_m$. And the acceleration of their diffusion can again be interpreted as due to an increase in partition coefficient with concentration.

Conclusion

The diffusion of bimodal polymer solutions through model porous membranes of pore radius $R_p = 75$ nm has been investigated as a function of concentration and solution composition in long and short chains.

In a dilute concentration regime, we have observed the existence of a semiequilibrium situation, with a concentration difference in short chains between the two compartments of a diffusion cell of opposite sign to the concentration difference in long chains. We attribute this to the large permeability difference of the membrane to the two molecular weights in solution. On an intermediate time scale, the short chains experience an expulsion due

to the retention of the long chains.

The diffusion kinetics of both species has been examined. In a dilute regime, it stays unchanged for both types of chain by the presence of another solute. Increasing the short chain concentration at fixed long chain concentration, we have observed an enhanced diffusion of the long chains. We interpret this effect as due to an increase of the long chain partition coefficient from the pores when short chains are added to the solution. A simple virial expansion model is in good quantitative agreement with our results, when the same parameters are used as in the analysis of single-chain diffusion kinetics presented in the accompanying paper.[1] The acceleration of the long chain diffusion is, however, less important by addition of short chains than by increase of long chain concentration. We show that this is due to the low exclusion of the short chains from the pores. The deswelling of the long chains by the short chains does not seem to play an important role in the explored concentration range. We have also observed in one experiment performed in an initial concentration regime of dilute short chains and overlapping long chains an acceleration of the short chain diffusion. We qualitatively attribute this effect to the fact that two driving forces should be effective in the presence of two solutes.

Acknowledgment. I thank P.-G. de Gennes for suggesting the experiments and critical reading of the manuscripts, F. Brochard, J. F. Joanny, L. Leibler, D. Broseta, D. Ausserré, and L. Léger for related discussions, and G. Chauveteau and M. Bagassi for communication of their results on transport under flow. I also acknowledge the help of P. Vidakovic and C. Sauterey for the ultracentrifugation experiments and L. Léger for the supply of the labeled polystyrene sample. These experiments have been made possible by the attribution of several irradiation periods at the A.L.I.C.E. heavy-ion accelerator in Orsay.

Registry No. Polystyrene, 9003-53-6; bisphenol A polycarbonate (copolymer), 25037-45-0; bisphenol A polycarbonate (SRU), 24936-68-3.

References and Notes

(1) Guillot, G. *Macromolecules*, preceding paper in this issue.
(2) Satterfield, C. N.; Colton, C. K.; De Turckheim, B.; Copeland, T. M. *AIChE J.* **1978**, *24*, 937.
(3) Schulz, J. S.; Valentine, R.; Choi, C. Y. *J. Gen. Physiol.* **1979**, *73*, 49.
(4) Cannell, D.; Rondelez, F. *Macromolecules* **1980**, *13*, 1599.
(5) Guillot, G.; Léger, L.; Rondelez, F. *Macromolecules* **1985**, *18*, 2531.
(6) Long, T. D.; Anderson, J. L. *J. Polym. Sci., Polym. Phys. Ed.* **1984**, *22*, 1261.
(7) Chauveteau, G.; Tirrell, M.; Omari, A. *J. Colloid Interface Sci.* **1984**, *100*, 41.
(8) Daoudi, S.; Brochard, F. *Macromolecules* **1978**, *11*, 751.
(9) De Gennes, P.-G. In *Scaling Concept in Polymer Physics*; Cornell University Press: Ithaca, NY 1979.
(10) Kedem, O.; Katchalsky, A. *Biochim. Biophys. Acta* **1958**, *27*, 229.
(11) Joanny, J. F.; Grant, P.; Turkevich, L. A.; Pincus, P. *J. Phys. (Les Ulis, Fr.)* **1981**, *42*, 1045; *J. Appl. Phys.* **1981**, *52*, 5943.
(12) Guillot, G.; Rondelez, F. *J. Appl. Phys.* **1981**, *52*, 7155.
(13) Léger, L.; Hervet, H.; Rondelez, F. *Macromolecules* **1981**, *14*, 1732.
(14) Lesec, J. Ecole Supérieure de Physique et Chimie, Paris, private communication.
(15) Vidakovic, P.; Rondelez, F. *Macromolecules* **1985**, *18*, 700.
(16) Schachman, H. K. *Ultracentrifugation in Biochemistry*; Academic: New York, 1959.
(17) Williams, J. W.; van Holde, K. E.; Baldwin, R. L.; Fujita, H. *Chem. Rev.* **1958**, *58*, 715.
(18) Flory, P. J. *J. Chem. Phys.* **1949**, *17*, 303.
(19) De Gennes, P.-G. *J. Polym. Sci., Polym. Symp.* **1977**, *61*, 313.
(20) Daoud, M.; de Gennes, P.-G. *J. Phys. (Les Ulis, Fr.)* **1977**, *38*, 85.
(21) Flory, P. J.; Krigbaum, W. R. *J. Chem. Phys.* **1950**, *18*, 1086.
(22) Witten, T.; Prentis, J. J. *J. Chem. Phys.* **1982**, *77*, 4247.

Measurement of Chain Dimensions in Dilute Polymer Solutions: A Light Scattering and Viscometric Study of Linear Polyisoprene in Cyclohexane

N. S. Davidson,† L. J. Fetters, W. G. Funk, N. Hadjichristidis,‡ and W. W. Graessley*

Corporate Research—Science Laboratories, Exxon Research and Engineering Company, Annandale, New Jersey 08801. *Received October 2, 1986*

ABSTRACT: Several methods for obtaining the size of macromolecules in dilute solution were applied to a series of linear polyisoprenes in the thermodynamically good solvent cyclohexane. The polymers, prepared by anionic polymerization, cover a wide range in molecular weight ($1.5 \times 10^4 < M < 3.4 \times 10^6$) and have narrow molecular weight distributions ($\bar{M}_w/\bar{M}_n < 1.1$). The viscometric radius R_V, the radius of gyration R_G, the hydrodynamic radius R_H, and the thermodynamic radius R_T were determined by viscometry and by static and dynamic light scattering. The molecular weight dependences of all four size measures are well-described by power laws ($R \propto M^a$). The exponents obtained for R_H, R_V, and R_T agree fairly well with the predicted value of 0.588 for good solvents. The exponent obtained for R_G is smaller, although R_G/R_H in fact changes rather little over the range of available data. The values of R_G/R_H, R_V/R_H, and R_T/R_H are in reasonable accord with the theory for self-avoiding coils and with results for polystyrene and poly(α-methylstyrene) in good solvents.

Introduction

Several methods are available for determining the size of polymer molecules in dilute solution. Some provide the radius of gyration R_G (angular dependence of light or neutron scattering intensity[1,2]), others the hydrodynamic radius R_H (diffusion[3,4] and sedimentation coefficients[5]) or some combination of R_G and R_H (intrinsic viscosity[6]), and still others a thermodynamic or excluded volume radius R_T (second virial coefficient in good solvents[6,7]). Such data are used extensively to test dilute solution theories predicting the influence of chain length, chain architecture,

† Present address: Research and Development Department, B.P. Chemicals Ltd., Grangemouth FK3 9XH, United Kingdom.
‡ Permanent address: Division of Chemistry, University of Athens, 10680 Athens, Greece.

0024-9297/87/2220-2614$01.50/0